Pathogenic Pathways in Fluconazole-Induced Branchial Arch Malformations

Elena Menegola, Maria L. Broccia, Francesca Di Renzo, and Erminio Giavini*

Department of Biology, University of Milan, Milan, Italy

Received 17 June 2002; Revised 16 September 2002; Accepted 30 September 2002

BACKGROUND: A widely-used antimycotic agent, bis-triazole fluconazole (FLUCO), is able to produce abnormalities to the branchial apparatus (hypoplasia, agenesis, and fusion) in postimplantation rodent embryos cultured in vitro. The branchial apparatus is a complex and transient structure in vertebrate embryos and is essential for the development of the face skeleton. Branchial arch mesenchyme is formed by two different cellular populations: paraxial mesenchyme and ectomesenchyme, which originate from rhombencephalic neural crest cell (NCC) migration. We investigated the possible pathogenic pathways involved in FLUCO-related branchial arch abnormalities. Perturbations in physiological apoptosis, cell proliferation, NCC migration and branchial mesenchyme induction have been considered. **METHODS:** Rat embryos (9.5-day postcoitum; 1–3 somites) were exposed in vitro to 0 or 500 μM FLUCO. After 24, 36, or 48 hr of culture, embryos were examined for apoptosis (acridine orange method) and cell proliferation (BrdU incorporation and detection method). Rhombencephalic NCC migration was analyzed using immunostaining of NCC (using anti-CRABP antibodies) and the extracellular matrix (using anti-fibronectin antibodies). The differentiative capability of the branchial mesenchymes was investigated using anti-endothelin and anti-endothelin-receptor antibodies. **RESULTS:** During the whole culture period, no alterations in physiological apoptosis, cell proliferation, and mesenchymal cell induction were observed in FLUCO-exposed embryos in comparison to controls. On the contrary, severe alterations in NCC migration pathways were observed in FLUCO-exposed embryos. **CONCLUSIONS:** The findings suggest that FLUCO produces teratogenic effects by interfering with the cellular and molecular mechanisms that control NCC migration. *Birth Defects Research (Part A) 67:116–124, 2003.* © 2003 Wiley-Liss, Inc.

INTRODUCTION

The bis-triazole derivative fluconazole (FLUCO) is an antifungal agent used clinically against vaginal, oropharyngeal and cutaneous candidiasis, disseminated candidiasis, and coccidioidal meningitis. The use of FLUCO for prophylaxis and treatment of mycotic infections is also widespread among pregnant women. The major routes of administration are oral and intravenous. Vaginal candidiasis is treated usually with a 150-mg single dose; oropharyngeal and esophageal candidiasis are generally treated for weeks or months with 50–150 mg FLUCO daily. Higher doses (200–400 mg daily) for long periods are used to treat deep mycoses (meningitis, ophthalmitis, pneumonia, hepatosplenic mycosis, endocarditis), whereas systemic mycoses are treated for several months with 400 mg FLUCO daily, respecting the total maximum daily recommended dose of 1,600 mg.

Despite the extensive use of FLUCO, the effects on the embryo and fetus have been only partially evaluated. Animal in vivo studies have shown that high doses of FLUCO can be teratogenic (Tachibana et al., 1987; Van Cauteren et al., 1990) with the observed abnormalities including craniofacial defects, although contrasting data are available about the effects of the drug in human pregnancy. In fact, prospective studies revealed no increase in birth defects after exposure to FLUCO (Imman et al., 1994; Mastroiacovo et al., 1996; Jick, 1999; Sørensen et al., 1999), whereas case-reports of long-term or high-dose maternal FLUCO therapy during pregnancy reported craniofacial abnormalities in newborns (Lee et al., 1992; Pursley et al., 1996; Aleck and Bartley, 1997; Sanchez and Moya, 1998). Animal in vitro studies on FLUCO have also been carried out using the rodent postimplantation whole embryo culture method (Tiboni, 1993; Menegola et al., 2001a). Mouse embryos exposed to about 150–250 μM FLUCO showed second branchial arch anomalies (Tiboni, 1993), and rat embryos exposed to 125–500 μM FLUCO showed severe alterations, specifically at the level of first and second branchial arches (hypoplasia, agenesis, and fusion) and at the level of maxillary processes (Menegola et al., 2001a). Similar abnormalities at the branchial apparatus level were described previously in rat embryos exposed in vitro to other triazole derivatives: triadimefon and triadimenol (Menegola at al., 2000) and flusilazole (Menegola et al., 2001a), showing that the branchial apparatus is the target of this chemical family.

In mammals, the branchial apparatus is a transient structure. At first, the branchial arches are composed basically of densely packed paraxial mesodermal cells (PMCs), surrounded by ectodermal and endodermal epithelia (Fig. 1).

*Correspondence to: Prof. Erminio Giavini, University of Milan, Department of Biology, Via Celoria, 26, 20133 Milan, Italy.
E-mail: erminio.giavini@unimi.it
Published online in Wiley InterScience (www.interscience.wiley.com).
DOI: 10.1002/bdra.10022

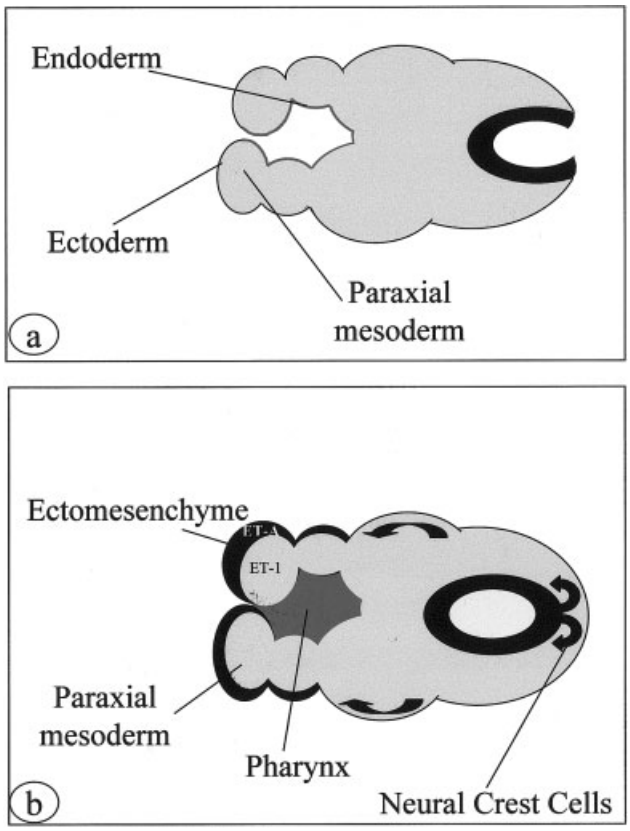

Figure 1. Scheme illustrating processes and cell populations involved in the morphogenesis of the branchial apparatus.

Later in embryogenesis, branchial arch mesenchyme is formed by two different cellular populations: paraxial mesenchyme and ectomesenchyme (Trainor and Tam, 1995). Viewing the craniofacial morphogenesis step-by-step (Fig. 1), the process begins with rhombencephalic neural crest cell (NCC) migration into the pharyngeal mesenchyme. Cells from specific rhombomeres lose their cell–cell adhesion properties and interact with the surrounding extracellular matrix. In particular, fibronectin and laminin provide a ground substrate for the movement of NCCs from the rhombencephalon to the early branchial structure (Perris and Perrisinotto, 2000). At the branchial level, PMCs and NCCs instruct each other to initiate the correct morphogenetic program: NCCs form the ectomesenchyme that condenses peripherally, whereas the paraxial mesenchyme, segregated in the mesenchymal core of the arch, is formed from PMCs (Trainor and Tam, 1995). The signaling pathway involved in the normal craniofacial development is represented by endothelin (ET-1), produced by paraxial mesenchyme, and endothelin receptors (ET-A), expressed by ectomesenchyme (Kurihara et al., 1999). From the paraxial mesenchyme arise muscles, some skeletal elements, vascular tissues; from the ectomesenchyme originate connective and cartilaginous tissues as well as part of branchial cranial nerves and ganglia (Le Douarin, 1982; Kimmel et al., 1991). In adults, the embryonic pharyngeal skeleton corresponds to the visceral portion of the head skeleton (maxillary and mandibular bones, zygomatic and temporal bones, auditory ossicles, tympanic ring, hyoid and larynx cartilages) (Fig. 2).

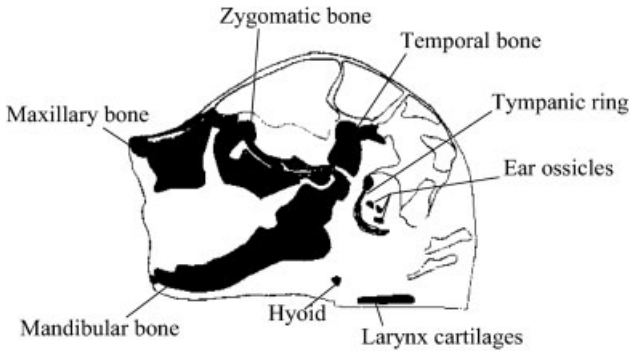

Figure 2. The pharyngeal skeleton: craniofacial derivatives of the embryonic branchial structures.

The specific effects observed at the craniofacial level after FLUCO in vivo exposure and at the branchial apparatus level after in vitro exposure focused our attention on the possible pathogenic pathways involved. Classic pathogenic pathways in teratological processes include perturbation in physiological apoptosis, cell proliferation, NCC migration and endothelin-mediated induction (Wilson, 1973) and they have been investigated in the present work. For this purpose, postimplantation rat embryos were exposed in vitro to 500 μM FLUCO (a concentration known to be teratogenic for 100% samples; Menegola et al., 2001a), cultured for 24, 36, or 48 hr, and processed to verify the specific objectives.

MATERIALS AND METHODS

Embryo Culture

Virgin female CD:Crl rats (Charles River, Calco, Italy), housed in a thermostatically-maintained room (T = 22 ± 2°C, relative humidity = 55 ± 5%) with a 12-hr light cycle (light from 6:00 AM to 6:00 PM), free access to food (Italiana Mangimi, Settimo Milanese, Italy) and tap water, were caged overnight with males of proven fertility. The morning of positive vaginal smear was considered Day 0 of gestation. Pregnant females were sacrificed on Day 9.5 postcoitum (p.c.), and embryos explanted under aseptic conditions. Embryos of 1–3 somites were selected and cultured according to the method proposed by New (1978) in 20-ml glass bottles (5 embryos/bottle), containing 5 ml of heat-inactivated sterile rat serum supplemented with antibiotics (100 IU/ml penicillin and 100 μg/ml streptomycin). Fluconazole (gift of Pfizer, Italy), dissolved in 100% ethanol, was added (5 μl/bottle) to obtain the concentration of 500 μM. In addition, a control and a control + ethanol (5 μl 100% ethanol/bottle) groups were carried out. The bottles, inserted in a thermostatic (38°C) roller (30 rpm) apparatus were gas-equilibrated periodically, according to Giavini et al. (1992). After 24, 36, or 48 hr in culture, the embryos were examined using a dissecting microscope and processed specifically for the different purposes.

Visualization of Apoptotic Cells

To visualize apoptotic cells, after 24 (Day 10.5 p.c.), 36 (Day 11 p.c.) or 48 (Day 11.5 p.c.) hours of culture, embryos

(at least six embryos per experimental point from at least three different bottles) were stained immediately with the vital dye acridine orange (Sigma, Italy; 5 μg/ml PBS), according to the method described by Abrams et al. (1993), washed three times in PBS, and viewed under a fluorescence microscope (EX = 490 nm). Using this method, physiologic and pathologic apoptotic areas were visible as fluorescent spots.

Cell Proliferation Analysis

To evaluate cellular proliferation, the BrdU incorporation method was applied; using the BrdU labeling and detection kit II (Boehringer, Mannheim, Germany). Two hours before the end of the culture (10.5, 11, or 11.5 day p.c.), 5 μl BrdU solution was added to 5 ml of culture medium. The samples (at least six embryos per experimental point from at least three different bottles) were fixed with 30% glycine in ethanol absolute, dehydrated, embedded in paraffin and sectioned. Histological sections (5μm) were rehydrated, washed in PBS, and incubated with the monoclonal antibody anti-BrdU overnight and washed again in PBS. After incubation with anti-mouse-Ig-alkaline phosphatase (1 hr) followed by washing in PBS, samples were incubated for 15 min with the substrate solution (nitroblue tetrazolium and 5-Br-4Cl-3-indolyl phosphate toluidinium) to allow the reaction. Cells that incorporated BrdU into DNA were then detected by light microscope as their nuclei were violet.

Whole-Mount Immunostaining of NCCs

To evaluate NCC migration, NCCs were immunostained specifically according to the method described by Wei et al. (1999). Briefly, after 24 (Day 10.5 p.c.), 36 (Day 11 p.c.) or 48 (Day 11.5 p.c.) hours of culture, embryos (at least six embryos per experimental point from at least three different bottles) were fixed in Dent's fixative (dimethyl sulfoxide: methanol, 1:4) overnight at -20°C. After washing in methanol and incubation with 5% H_2O_2 in methanol embryos were hydrated and incubated for 3 days at 4°C with the monoclonal antibody anti-CRABP, cellular retinoic acid binding proteins (ABR) expressed specifically at these embryonic stages by NCCs (Vaessen et al., 1989; Ruberte et al., 1991), diluted 1:500 in PBS. After washing and incubation with the anti-mouse-Ig-peroxidase (Fab fragment, Boehringer), diluted 1:40 in PBS, overnight at 4°C, staining was carried out with the substrate 4-Cl-1-naphtol (Sigma, St. Louis, MO) and 0.006% H_2O_2. Stained cells appeared dark brown through the light microscope.

Immunohistochemistry of NCC

After fixation with Dent's fixative (1:4 in vol dimethyl sulfoxide: methanol) overnight at -20°C, some embryos were embedded in paraffin and sectioned. After hydration, samples were washed in 0.3% H_2O_2 in distilled water and incubated at 4°C overnight with the monoclonal antibody anti-CRABP, diluted 1:500 in PBS, washed in PBS, incubated with the anti-mouse-Ig-peroxidase (Boehringer; 1 hr, diluted 1:40 in PBS), washed again and incubated for 30 sec with the substrate solution, diaminobenzidine (Sigma) and H_2O_2. Neural crest cells were detected by light microscopy, as their cytoplasm was brown.

Immunostaining of Fibronectin

Whole-mount immunostaining and immunohistochemistry of fibronectin were carried out after 36 and 48 hr of culture (11 and 11.5 day p.c.). After fixation in 3% paraformaldehyde dissolved in PBS (1 hr), embryos (at least six embryos per experimental point from at least three different bottles) were processed for whole-mount immunostaining or were embedded in paraffin and processed for immunohistochemistry. The applied method was quite similar to that reported above for NCC immunostaining. The primary antibody was a monoclonal antibody anti-fibronectin (Chemicon, Temecula, CA) diluted 1:300 in PBS. The secondary antibody was a anti-mouse-Ig-peroxidase (Boehringer, Mannheim, GE) diluted 1:40 in PBS.

Whole-Mount Immunostaining of ET-1 and ET-A

Whole-mount immunostaining of ET-1 and ET-A was carried out after 48 hr of culture (11.5 day p.c.). After fixation in 3% paraformaldehyde dissolved in PBS (6 hr at 4°C) (for ET-1) or in methanol overnight at -20°C (for ET-A), embryos were processed for whole-mount immu-

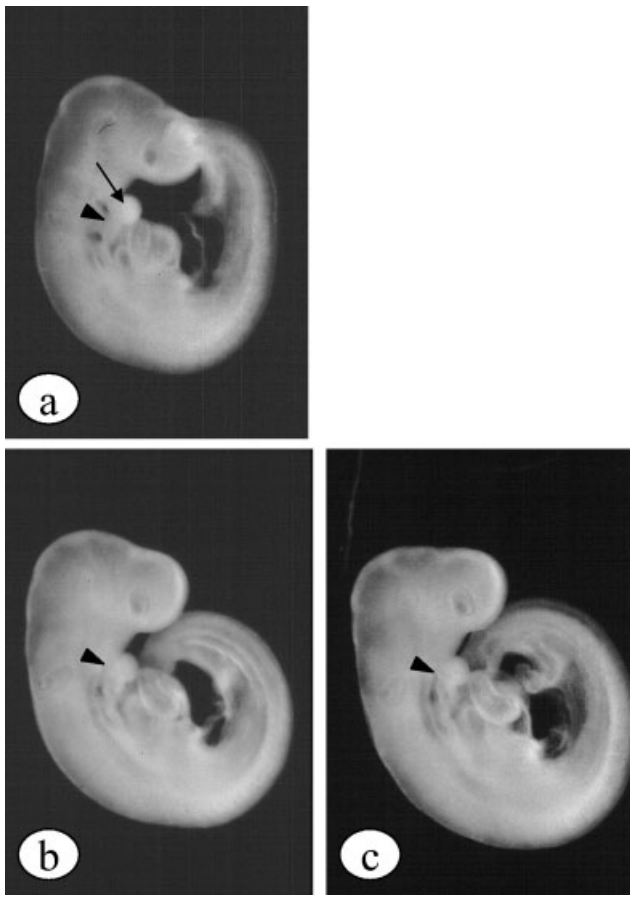

Figure 3. 11.5-day p.c. embryos. In control (**a**) note the developed and separated first (arrow) and second (arrowhead) branchial arches. (**b**, **c**) FLUCO-exposed embryos showing the typical abnormalities at the level of the branchial apparatus: first and second branchial arches partially (b) or completely fused (c) (arrowhead). Magnification: 25×.

nostaining. The applied method was similar to that mentioned above for NCC immunostaining. The primary antibodies were rabbit anti-ET-1,2,3 (Chemicon) diluted 1:250 in PBS, and rabbit anti-ET-A (Chemicon) diluted 1:50 in PBS. The secondary antibody was a anti-rabbit-Ig-peroxidase (Boehringer) diluted 1:40 in PBS.

RESULTS

After 24 hr of culture, all FLUCO-exposed embryos showed a developmental delay of the first branchial arch. After 36 and 48 hr in culture, 100% of embryos exposed to FLUCO showed malformations at the branchial apparatus level, with typical and similar malformations for all em-

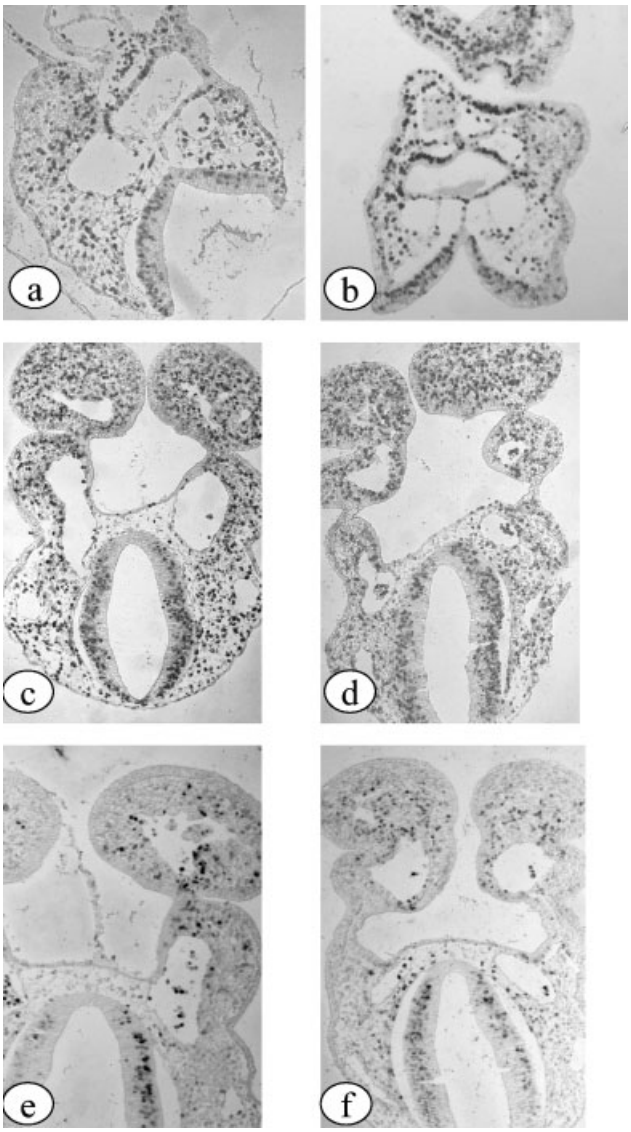

Figure 4. Appearance of embryonic slides after BrdU labeling: BrdU-positive cells exhibited violet nuclei. During the whole culture period (**a**,**b**: 10.5 days p.c.; **c**,**d**: 11 days p.c.; **e**,**f**: 11.5 days p.c.), a similar rate of cell proliferation was visible in FLUCO-exposed embryos in comparison to controls. Magnification: 25×.

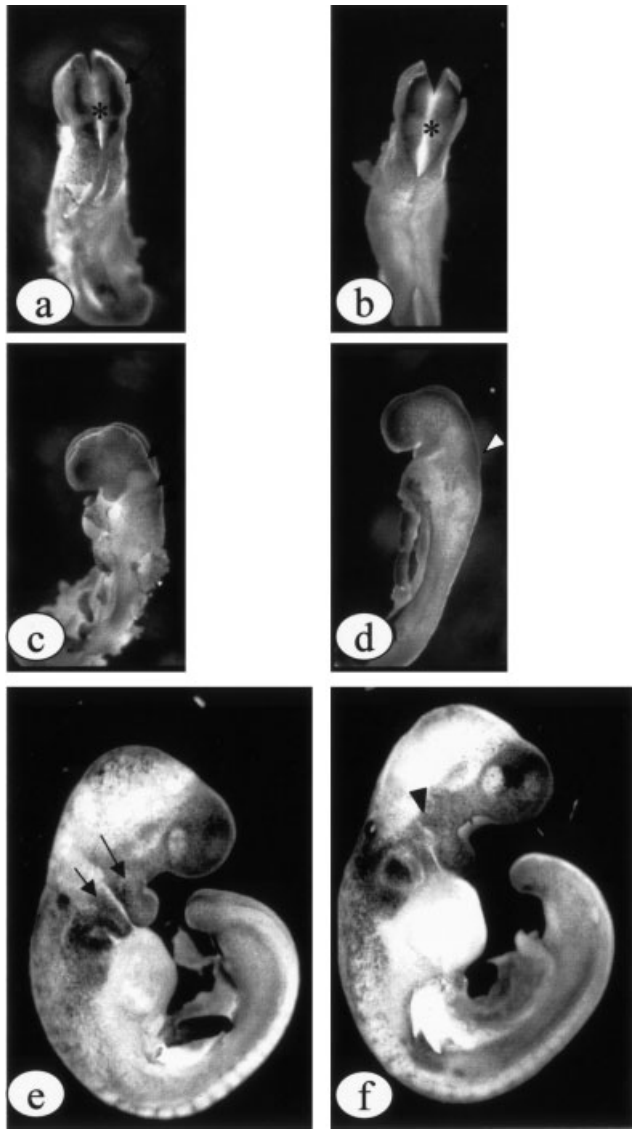

Figure 5. Control (**a**,**c**,**e**) and FLUCO-exposed embryos (**b**,**d**,**f**) after whole-mount CRABP immunostaining showing NCC distribution. (a–d) embryos 10.5 days p.c. old. (a,b) Dorsal view: the immunostained mass seems distributed along the rhombencephalic profile (arrow) both in control (a) and in FLUCO-exposed embryo (b). At this developmental stage, the rhombencephalon is open physiologically (asterisk). (c,d) Lateral view: at this embryonic stage NCC migration from the rhombencephalon to the branchial apparatus begins. Three characteristic strips (arrows) are visible in controls (c), directed to the pharyngeal region. A diffused CRABP-positive mass (arrowhead) was, on the contrary, detectable near the rhombencephalon in FLUCO-exposed embryos (d). Magnification: 40×. (e,f) Eleven days p.c. embryos, lateral view. At this developmental stage, NCCs are localized at the level of the branchial apparatus both in controls (e) and in FLUCO-exposed embryos (f). At the level of first and second branchial arch, NCCs formed an indistinguishable population (arrowhead) in FLUCO-exposed embryos (f) in comparison to controls (e) showing, on the contrary, well separated colonized areas (arrows). Magnification: 25×.

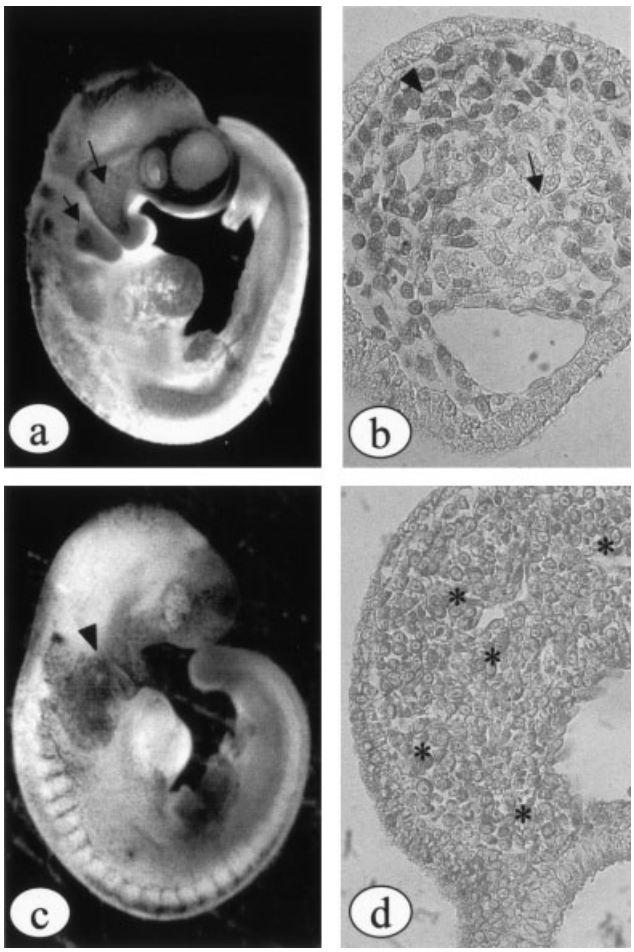

Figure 6. (**a**,**c**) Embryos 11.5 days p.c., after whole-mount CRABP immunostaining, showing NCC distribution at the level of the branchial apparatus. Magnification: 25×. At this embryonic stage, controls (a) showed NCC derived tissues condensed at the level of first and second branchial arches (arrows). On the contrary, in FLUCO-exposed embryos (c) NCC formed an indistinguishable population (arrowhead) unable to condense. (**b**,**d**) Histological appearance of branchial tissues after CRABP-positive cell immunolocalization. Magnification: 100×. In the control slide (b), it is possible to recognize two different tissues: paraxial mesenchyme (arrow) and ectomesenchyme (arrowhead, positive to the staining). The ectomesenchyme seems condensed at the marginal area of the branchial arch. FLUCO-exposed embryos (d), on the contrary, showed the ectomesenchymal tissue unable to condense, formed by positive cells (asterisks) mixed with the non positive paraxial mesenchymal cells.

bryos (hypoplasia of branchial arches and fusion between first and second branchial arches) (Fig. 3).

Visualization of Apoptotic Cells

The vital dye acridine orange method was used for the visualization of apoptotic areas. Physiological apoptosis was detectable both in controls and in FLUCO-exposed embryos at the level of the otic and optic vesicles and at the maxillary process level. No differences or increase in apoptotic areas were observed in FLUCO-exposed embryos compared to controls (data not shown).

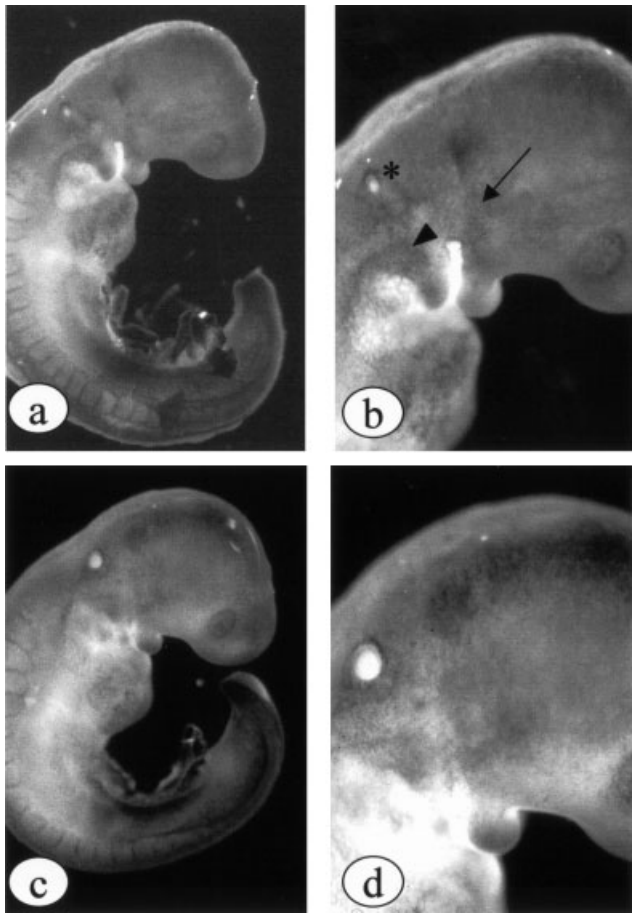

Figure 7. Whole-mount immunostaining of fibronectin. In controls (**a**,**b**) the fibronectin seemed typically distributed from the rhombencephalon to the first branchial arch (arrow), near the otic vesicle (asterisk) and from the second to the third branchial arches, forming a comma shape structure (arrowhead). On the contrary, in FLUCO-exposed embryos (**c**,**d**) a diffuse distribution of fibronectin was observed. Magnification: 25× (a,c), 30× (b), 40× (d).

Cell Proliferation Analysis

After BrdU labeling, a normal rate of cell proliferation was visible in all embryonic tissues both in controls and in FLUCO-exposed embryos during the whole culture period (Fig. 4).

NCC Migration Analysis

For the visualization of NCCs, CRABP immunostaining of used. At 10.5 days p.c., NCCs were visible along the rhombencephalic profile both in controls and in FLUCO-exposed embryos (Fig. 5a,b). The lateral view of embryos allowed us to identify a clear stain at the level of the nasal mesenchyme in controls, and three distinct positive strips connecting the rhombencephalic region to the pharyngeal region (at this developmental stage, only the first branchial arch is partially formed and appeared faintly immunostained). Embryos exposed to FLUCO showed the stain at the nasal mesenchyme (as in controls). On the contrary, the three distinct positive strips connecting the rhombencephalic region to the pharyngeal region were absent in

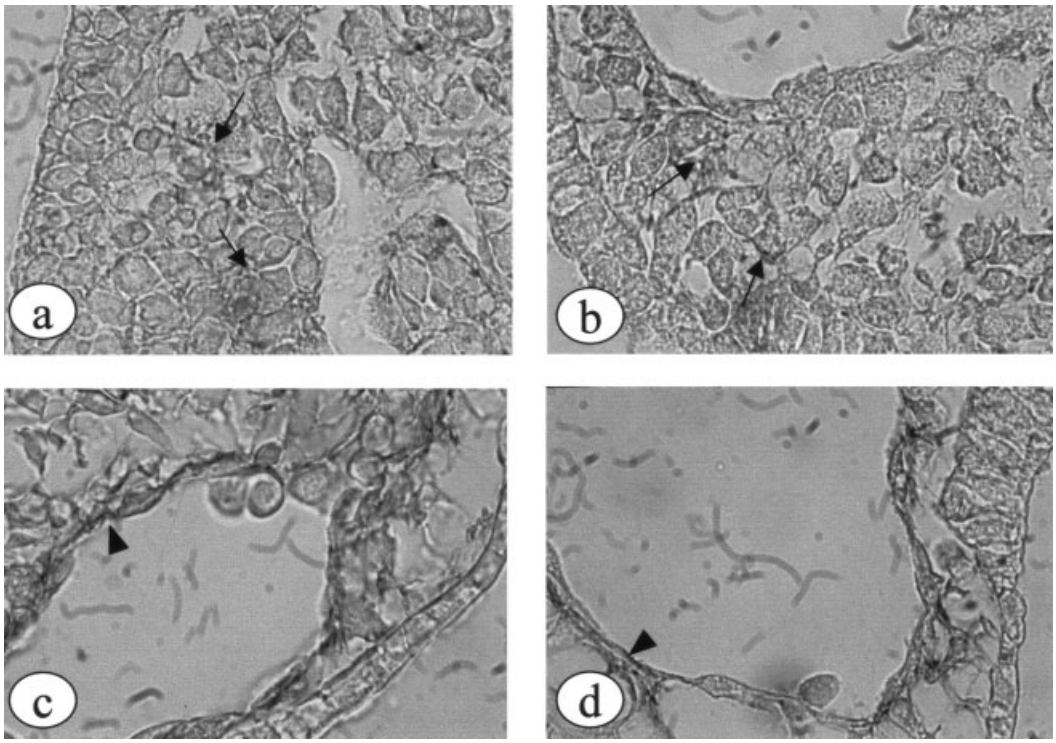

Figure 8. Immunohistochemical localization of fibronectin in controls (**a**,**c**) and in FLUCO-exposed embryos (**b**,**d**) at the level of the first branchial arch (a,b) and of the dorsal aorta (c,d). Both in controls and in FLUCO-exposed embryos, the diffused fibronectin extracellular localization (arrows) at the branchial arch level and the clear immunoreactivity at the aortic basal lamina (arrowhead) were observed. Magnification: 1000×.

exposed embryos, but a diffused CRABP-positive mass was detectable near the rhombencephalon (Fig. 5c,d).

At 11 days p.c., NCCs had migrated into the branchial mesoderm, in both controls and FLUCO-exposed embryos. At the level of first and second branchial arch, NCCs seemed to be separated well in controls, whereas they formed an indistinguishable population in FLUCO-exposed embryos (Fig. 5e,f). Finally, at 11.5 days p.c., FLUCO-exposed embryos showed the ectomesenchymal tissue unable to condense, forming a continuos positive mass diffused along the branchial apparatus (Fig. 6a,c). The immunohistochemical localization of NCCs showed positive cells in controls and in FLUCO-exposed embryos. At 11.5 days p.c., their distribution into the branchial arches of control embryos showed a normal pattern: NCCs localized at the marginal zone only, whereas the core was occupied by PMCs. In FLUCO-exposed embryos, however, NCCs and PMCs were mixed into the branchial arches without any regionalization (Fig. 6b,d).

After whole-mount immunostaining of fibronectin, the distribution of extracellular matrix was visualized after 36 and 48 hr in culture (11 and 11.5 days p.c.). Both controls and FLUCO-exposed embryos showed immunoreactivity to the antibody. At the branchial apparatus level, fibronectin distribution seemed typical in controls (from the rhombencephalon to the first branchial arch, near the otic vesicle and with a comma shape connecting the second and third branchial arches) (Fig. 7a,b). This typical distribution was completely absent in FLUCO-exposed embryos, where a diffuse distribution of fibronectin was observed (Fig. 7c,d). The immunohistochemical localization of fibronectin showed the extracellular matrix as positive, particularly at the level of the vessel basal laminae, both in controls and in FLUCO-exposed embryos (Fig. 8).

Immunostaining of ET-1 and ET-A

The immunostaining of embryos with antibodies, anti-endothelin and its receptor ET-A seemed quite similar to each other in controls. The areas stained were the nasal mesenchyme, the trigeminal area, the otic area, the branchial arches, and the heart (Figs. 9a,b, 10a,b). In embryos exposed to FLUCO, the positive areas were similar to controls (nasal region, otic region, and heart) but a diffuse immunostained mass was visible from the trigeminal region throughout the branchial apparatus. (Figs. 9c,d, 10c,d).

DISCUSSION

The teratogenic potential of FLUCO on postimplantation rat whole embryo cultures was confirmed by this work: the observed specific abnormalities at the level of the branchial apparatus are in agreement with our previous data on in vitro effects of triazole-derivatives (Menegola et al., 2001a), where FLUCO produced specific branchial arch abnormalities in a concentration-related manner. In this study, the FLUCO concentration used (500 μM, about five times the maximum plasma level reported in pregnant women exposed to 800 mg/day FLUCO) produced, as expected, 100% of branchial arch abnormalities.

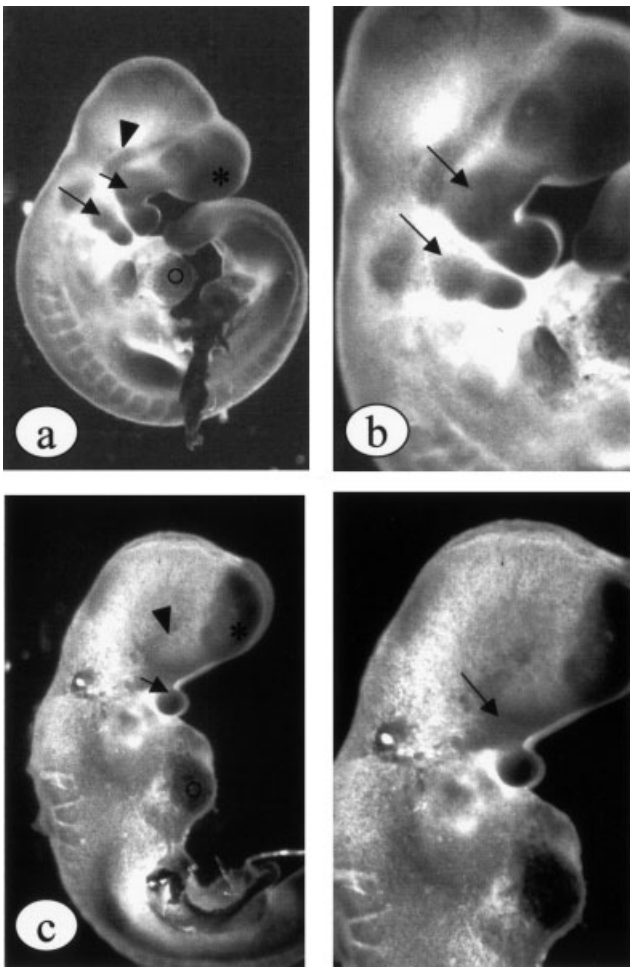

Figure 9. Whole-mount immunolocalization of endothelin (ET-1). (**a**,**b**) Control: note the clear stain of the nasal mesenchyme (asterisk), the trigeminal area (arrowhead), the branchial arches (arrows) and the heart (circle). (**c**,**d**) FLUCO-exposed embryo: the ET-1 distribution is similar to controls but a diffuse immunostained mass is visible at the level of the malformed branchial arches (arrow). Magnification: 25× (a,c); 40× (b,d).

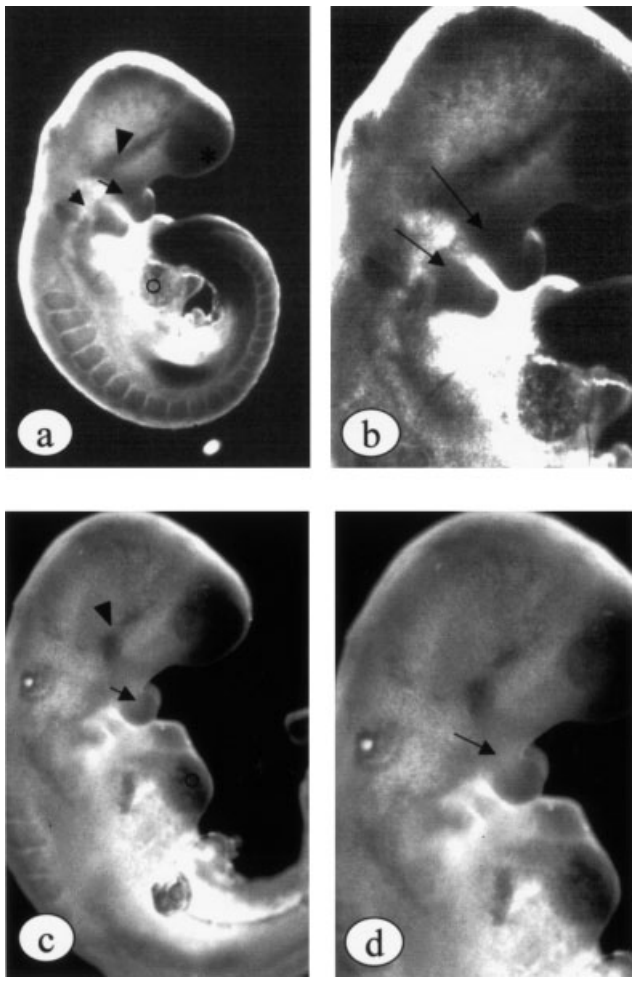

Figure 10. Whole-mount immunolocalization of the endothelin receptor ET-A in a control embryo (**a**,**b**) and in a FLUCO-exposed embryo (**c**,**d**). Similar to the observation shown for the endothelin, the ET-A localization in FLUCO-exposed embryos is similar to controls, at the level of the nasal mesenchyme (asterisk), the trigeminal area (arrowhead), the branchial apparatus (arrows) and the heart (circle), but in FLUCO-exposed embryos at the level of the malformed branchial arches (arrow), a diffuse immunostained mass is visible. Magnification: 25× (a,c); 40× (b,d).

Craniofacial morphogenesis is a complex phenomenon based on the active interaction between different tissues forming the branchial apparatus. The tissues involved are the paraxial mesenchyme and the ectomesenchyme, which have different embryologic (the first arises from the primitive mesodermal layer, the second from the neuroectoderm) and anatomic (the one from the pharyngeal region, the other from the dorsal region) origins. Pharyngeal morphogenesis can be summarized in seven principal steps: 1) proliferation of the PMC, forming the primitive branchial bars; 2) detachment of NCCs from the rhombencephalic epithelium; 3) migration of NCCs on extracellular guiding cues; 4) neural crest cell colonization of the branchial arch territories; 5) neural crest cell condensation forming a compact ectomesenchyme; 6) segregation of the paraxial mesenchyme into the core of the branchial arches; and 7) induction of the ectomesenchyme by the endothelin signal produced from the paraxial mesoderm. Deviation of one or more of these morphogenetic processes can lead to alterations to the craniofacial structures.

Severe head skeleton alterations have been well documented after exposure to several teratogenic agents: ethanol (Abel, 1984), retinoic acid (Lammer et al., 1985), folic acid antagonists (Warkany, 1978), diphenylhydantoin (Adams et al., 1990), hyperthermia (Pleet et al., 1981), and hypoxia (Millicovsky and Johnston, 1981). In some cases, pathogenic pathway involved has been documented: ethanol exposure triggers pathologic cell death (Kotch and Sulik, 1992; Menegola et al., 2001b), retinoids alter the NCC migration from rhombomeres (Webster et al., 1986; Granstrom and Kullaa-Mikkonen, 1990).

The aim of the present work was to investigate some of the pathogenic pathways probably involved in FLUCO-related teratogenesis. Perturbation in physiologic apopto-

sis, cell proliferation, NCC migration and endothelin-mediated induction have been considered.

As far as apoptosis, cell proliferation, and endothelin-mediated induction are concerned, no differences were observed between controls and FLUCO-exposed embryos during the whole culture period. Consequently, these processes do not seem to be involved in FLUCO-related embryopathies.

On the contrary, severe changes in the distribution of NCCs at the level of the branchial apparatus have been observed in FLUCO-exposed embryos. The immunostained mass, visible on Day 10.5 p.c. along the rhombencephalic profile, reached the target structures both in controls and in FLUCO-exposed embryos at the end of the culture period. This result suggests that the NCC motility was not compromised by FLUCO-exposure. The migration pathway, however, seemed deeply disrupted from 10.5 days p.c. on: NCCs of FLUCO-exposed embryos, on 10.5 days p.c., were not migrating into the three distinct strips, connecting the rhombencephalic origin sites to the target structures (Fig. 5c,d), and showed, on 11 and 11.5 days p.c., an abnormal reciprocal distribution of branchial tissues (Figs. 5e–h, 6). This abnormal organization also accounts for the altered appearance of the distribution of the extracellular matrix and the distribution of tissues producing endothelin and expressing the endothelin receptor, which have to be considered a consequence and not the cause of the altered NCC migration pattern. The extracellular accumulation of fibronectin and laminin, in fact, is controlled by the migrated NCCs themselves (Bronner-Fraser, 1993). The detected abnormal localization of fibronectin could only reflect the abnormal spatial organization of NCC-derivative tissues. On the other hand, differentiation of tissues producing ET-1 and expressing ET-A is a process starting when NCCs reach the final localization at the level of the branchial structures. Viewing the process step-by-step: the abnormal colocalization of NCCs and lateral mesenchyme at the branchial level could lead to the consequent abnormal colocalization of the differentiated ectomesenchyme and paraxial mesenchyme, producing ET-1 and ET-A.

In chick and other vertebrate embryos during hindbrain segmentation, NCCs delaminate from specific rhombomeres and migrate along segmental pathways to colonize the branchial arches. Hindbrain-derived neural crest cells migrate generally as three distinct streams adjacent to rhombomeres 2, 4, and 6, contributing to the first, second, and third branchial arches, respectively (Osumi-Yamashita et al., 1994; Trainor and Tam, 1995; Kulesa and Fraser, 2000). In contrast, there are clear neural crest-free zones adjacent to rhombomeres 3 and 5. Considering this specific migration pathway, the pattern of NCC localization observed in Day 10.5 p.c. embryos after FLUCO-exposure suggests an interference with the regular hindbrain segmentation in forming the rhombomeres, and a consequent altered distribution of NCCs into branchial arch mesenchyme. Similar patterns have been observed after exposure of rodent embryos to retinoic acid (Webster et al., 1986; Lee et al., 1995), the endogenous morphogen that regulates the expression of the Hox genes controlling the hindbrain segmentation. The hypothesis that triazole-derivatives may produce their effects through an alteration of the hindbrain is not to be excluded. The related mechanism could be mediated by interference with endogenous retinoic acid metabolism, as suggested by the observation that some triazoles can inhibit retinoic acid metabolism (Van Wauwe et al., 1990; Schwartz et al., 1995).

In conclusion, the exposure of rat embryos in vitro to 500μM FLUCO produced 100% abnormal embryos with abnormalities at the level of branchial arch apparatus. These abnormalities were not related with increased apoptosis, alteration of cell proliferation, or to abnormal mesenchymal cell induction. Severe alterations in NCC migration pathways were observed in all embryos exposed to FLUCO. These finding suggest that FLUCO produces its effects by interfering with the cellular and molecular mechanisms that control NCC migration.

REFERENCES

Abel EL. 1984. Fetal alcohol syndrome and fetal alcohol effects. New York: Plenum Press.

Abrahams JM, White K, Fessler LI, Steller H. 1993. Programmed cell death during Drosophila embryogenesis. Development 117:29–43.

Adams J, Vorhees CV, Middaugh LD. 1990. Developmental neurotoxicity of anticonvulsants: human and animal evidence on phenytoin. Neurotoxicol Teratol 12:203–214.

Aleck KA, Bartley DL. 1997. Multiple malformation syndrome following fluconazole use in pregnancy: report of an additional patient. Am J Med Genet 72:253–256.

Bronner-Fraser M. 1993. Cell interactions in neural crest cells migration. Adv Dev Biol 2:119–152.

Giavini E, Broccia ML, Prati M, Bellomo D, Menegola E. 1992. Effects of ethanol and acetaldehyde on rat embryos developing in vitro. In Vitro Cell Dev Biol 28:205–210.

Granstrom G, Kullaa-Mikkonen A. 1990. Experimental craniofacial malformations induced by retinoids and resembling branchial arch syndrome. Scand J Plastic Reconstr Surg Hand Surg 24:3–12.

Imman W, Pearce G, Wilton L. 1994. Safety of fluconazole in the treatment of vaginal candidiasis. Eur J Clin Pharmacol 46:115–118.

Jick SS. 1999. Pregnancy outcomes after maternal exposure to fluconazole. Pharmacotherapy 19:221–222.

Kimmel CB, Schilling TF, Hatta K. 1991. Patterning of body segments of the zebrafish embryo. Curr Top Dev Biol 25:77–110.

Kotch LE, Sulik KK. 1992. Experimental fetal alcohol syndrome: proposed pathogenic basis for a variety of associated craniofacial and brain anomalies. Am J Med Genet 44:168–176.

Kulesa PM, Fraser SE. 2000. In ovo time-lapse analysis of chick hindbrain neural crest cell migration shows cell interaction during migration to the branchial arches. Development 127:1161–1172.

Kurihara H, Kurihara Y, Nagai R, Yazaki Y. 1999. Endothelin and neural crest development. Cell Mol Biol 45:639–651.

Lammer EJ, Chen DT, Hoar RM, Agnish ND, Benke PJ, Braun JT, Curry CJ, Fernhoff PM, Grix AW Jr, Lott IT, Richard JM, Sun SC. 1985. Retinoic acid embryopathy. N Engl J Med 313:837–841.

Le Douarin NM. 1982. The neural crest. New York: Cambridge University Press.

Lee BE, Feinberg M, Abraham J, Murthy ARK. 1992. Congenital malformations in an infant born to a woman treated with fluconazole. Pediatr Infect Dis J 11:1062–1063.

Lee YM, Osumi-Yamashita N, Ninomiya Y, Moon CK, Eriksson U, Eto K. 1995. Retinoic acid stage-dependently alters the migration pattern and identity of hindbrain neural crest cells. Development 121:825–837.

Mastroiacovo P, Mazzone T, Botto LD, Serafini MA, Finardi A, Caramelli L, Fusco D. 1996. Prospective assessment of pregnancy outcomes after first-trimester exposure to fluconazole. Am J Obstet Gynecol 175:1645–1650.

Menegola E, Broccia ML, Di Renzo F, Prati M, Giavini E. 2000. In vitro teratogenic potential of two antifungal triazoles: triadimefon and triadimenol. In Vitro Cell Dev Biol 36:88–95.

Menegola E, Broccia ML, Di Renzo F, Giavini E. 2001a. Antifungal triazoles induce malformations in vitro. Reprod Toxicol 15:421–427.

Menegola E, Broccia ML, Di Renzo F, Giavini E. 2001b. Acetaldehyde in vitro exposure and apoptosis: a possible mechanism of teratogenesis. Alcohol 23:35–39.

Millicovsky G, Johnston MC. 1981. Hyperoxia and hypoxia in pregnancy: simple experimental manipulation alters the incidence of cleft lip and palate in CL/Fr mice. Proc Natl Acad Sci USA 9:5722–5723.

New DAT. 1978. Whole embryo culture and the study of mammalian embryos during organogenesis. Biol Rev 53:81–122.

Osumi-Yamashita N, Ninimiya Y, Doi H, Eto K. 1994. The contribution of

both forebrain and midbrain crest cells to the mesenchyme in the frontonasal mass of mouse embryos. Dev Biol 164:409–419.
Perris R, Perrisinotto D. 2000. Role of the extracellular matrix during neural crest cell migration. Mech Dev 95:3–21.
Pleet H, Graham JM, Smith DW. 1981. Central nervous system and facial defects associated with maternal hyperthermia at 4 to 14 weeks' gestation. Pediatrics 67:785–789.
Pursley TJ, Blomquist IK, Abraham J, Andersen HF, Bartley JA. 1996. Fluconazole-induced congenital anomalies in three infants. Clin Infect Dis 22:336–340.
Ruberte E, Dollé P, Chambon P, Morris-Kay G. 1991. Retinoic acid receptors and cellular retinoid binding proteins II. Their differential pattern of transcription during early morphogenesis in mouse embryos. Development 111:45–60.
Sanchez JM, Moya G. 1998. Fluconazole teratogenicity. Prenat Diagn 18: 862–869.
Schwartz EL, Hallam S, Gallagher RE, Wiernik PH. 1995. Inhibition of all-trans retinoic acid metabolism by fluconazole in vitro and in patients with acute promyelocytic leukemia. Biochem Pharmacol 7:923–928.
Sørensen HT, Nielsen GL, Olesen CO, Larsen H, Steffensen FH, Schønheyder HC, Olsen J, Czeisel AE. 1999. Risk of malformations and other outcomes in children exposed to fluconazole in utero. J Clin Pharmacol 48:234–238.
Tachibana M, Noguchi Y, Monro AM. 1987. Toxicology of fluconazole in experimental animals. In: Fromtling RA, editor. Recent trends in the discovery, development, and evaluation of antifungal agents. Barcelona, Spain: J Proust Science Publishers. pp. 93–102.
Tiboni GM. 1993. Second branchial arch anomalies induced by fluconazole, a bis-triazole antifungal agent, in cultured mouse embryos. Res Commun Chem Pathol Pharmacol 79:381–384.
Trainor PA, Tam PPL. 1995. Cranial paraxial mesoderm and neural crest cells of the mouse embryo: co-distribution in the craniofacial mesenchyme but distinct segregation in branchial arches. Development 121: 2569–2582.
Vaessen MJ, Kootwijk E, Mummery C, Hiekens T, Bootsma D, Van Kessel AD. 1989. Preferential expression of cellular retinoic acid binding protein in a subpopulation of neural cells in the developing mouse embryo. Differentiation 40:99–105.
Van Cauteren AL, Vandenberghe J, Vanparys P, Coussement W, De Coster R, Marsboom R. 1990. Safety aspects of oral antifungal agents. Br J Clin Pract 44:47–49.
Van Wauwe JP, Coene MC, Goossens J, Cools W, Monbaliu J. 1990. Effects of cytochrome P-450 inhibitors on the in vivo metabolism of all-trans retinoic acid in rats. J Pharmacol Exp Ther 252:365–369.
Warkany J. 1978. Aminopterin and methotrexate: folic acid deficiency. Teratology 17:353–358.
Webster WS, Johnston MC, Lammer EJ, Sulik KK. 1986. Isotretinoin embryopathy and the cranial neural crest: an in vivo and in vitro study. J Craniofac Genet Dev Biol 6:211–222.
Wei X, Makori N, Peterson PE, Hummler H, Hendrickx AG. 1999. Pathogenesis of retinoic acid-induced ear malformations in a primate model. Teratology 60:83–92.
Wilson JG. 1973. Environment and birth defects. New York: Academic Press. pp. 97–109.